# Experimental and numerical analysis of 7075 aluminum alloy fracture behavior

M. POP*, D. FRUNZA, F. POPA, A. NEAG
*Technical University, Faculty of Materials Engineering and Environment, B-dul Muncii 103-105, Cluj-Napoca, Romania*

The ductility and fracture behavior of an extruded 7075 aluminum alloy was studied using the tensile testing method in a wide range of temperatures (300–450°C) and strain rates ($10^{-1}$-$10^{-3}s^{-1}$). The results indicated that the ductility was monotonically increased by increasing deformation temperature. This was justified considering the fact that the volume fractions of the second phase particles might decrease at higher temperature thereby their detrimental effects on cavity nucleation and growth would be decreased. The normalized Cockcroft and Latham ductile fracture criterion used in the finite element analysis shown the critical damage value for the studied material.

(Received September 17, 2015; accepted October 28, 2015)

*Keywords:* Aluminum alloy; Hot ductility; Fractography; Numerical simulation

## 1. Introduction

Bulk metalworking processes are carried out at elevated temperatures where the occurrence of simultaneous softening process would enable the imposition of large strains in a single step or

multiple steps. Hot working also causes a significant change in the microstructure of the material and this contributes to one part of workability generally referred to intrinsic workability, which is sensitive to initial conditions and the process parameters [1].

Failure by surface or internal cracking in bulk metal forming is caused by the accumulation of ductile damage within regions that are highly strained due to extensive plastic flow. Apart from special purpose processes such as the shearing of bars and bar sections, where cracks are needed to cut material, the occurrence of cracks is generally undesirable and should be prevented during process design [ 2]. The 7000 aluminum series are very attractive materials to be employed in the automotive and aerospace industries. This is mainly due to their excellent combination of properties such as high strength to density ratio, fracture toughness, and resistance to stress corrosion cracking (SCC) [3,4].

The growing applications of aluminum alloys in both the aerospace and automotive industries have brought great challenges manifested in understanding material behavior.

In the case of Al-Zn-Mg-Cu alloys, as the most common high strength precipitation-hardened aluminum alloys, the elongation properties at room temperature appear to be the main problem to properly industrialize the desired forming processes.

The low formability can be slightly improved through applying homogenization treatment prior to forming. From the manufacturing point of view, conducting a proper thermomechanical processing (TMP) route is essential. It is well established that the hot deformation behavior and microstructural evolution of these alloys are very sensitive to TMP parameters. In fact, these wrought alloys may contain a large fraction of second phase precipitates distributing either in grain interiors or at the grain boundaries; this introduces a significant effect on ductility behavior of the material. According to the all aforementioned facts it is concluded that the hot ductility behavior and the optimum deformation conditions of Al-Zn-Mg-Cu alloys are strongly influenced by a variety of parameters such as grain size, strain rate, presence of grain boundary particles, deformation mode, and so on. Therefore the investigation of mechanical behavior and microstructural evolution of these alloys during hot deformation would assist clarifying their workability behavior[5,6].

The fracture behaviour of high-strength age hardening alloys has been extensively studied during the last several decades [7,8,9]. The complex and inhomogeneous microstructure is formed during processing and is unique for the various production processes. The fracture behaviour will be different for materials processed by rolling, extrusion or forging. In addition, the heat treatment these alloys are exposed to will change the microstructure, such as the grain morphology, the particle size and distribution, and the crystallographic texture, and thus significantly affect the fracture behaviour [10]. Age hardening aluminum alloys form precipitates, precipitation free zones, grain boundary precipitates and grains with different shapes during processing [11].

The present work deals with the deformation behavior and microstructural evolution of A7075-T6 aluminum alloy upon tension testing at elevated temperatures (above 300 $^0$C). The fracture surfaces were also analysed by scanning electron microscopy in order to justify them through the associated deformation mechanisms. Also the distribution of the main parameters of the process and the ductile fracture criterion were determined according to a simulation analysis.

## 2. Theoretical aspects

In the metal forming process, because of plastic deformation, large defects in a workpiece appear due of its ductility. Brittle fractures of metallic materials appear in the grain boundary surface between split atoms combined with each other. Ductile failure is partly caused by the crystalline grain boundary sliding caused by shear damage and also because of processing parameters such as the strain rate, temperature and lubrication. Ductile fracture is a limiting factor in cold and hot metal forming processes. For sheet metal forming, predictions of local necking that leads to fracture are usually based on the concept of a forming limit diagram in terms of major and minor principal strains has shown that the hydrostatic stress is of great importance [12,13].

In literature, there exist several criteria suggesting various ways of calculating critical damage values to detect crack initiations. The basic idea of many ductile fracture criteria is that fracture occurs when the value of a damage parameter reaches a critical value. The critical value at which fracture initiates varies substantially from material to material, and can even vary for a given material with different annealing treatments. Typical criteria for ductile fracture are usually based on combinations of stress with strain or strain rate, rather than on either of these quantities separately[14,15].

All the integrated stress–strain criteria based on empirical and semiempirical approach are versions of Freudenthal's critical plastic work per unit of volume,

$$\int_0^{\bar{\varepsilon}_f} \bar{\sigma}\, d\,\bar{\varepsilon} = C_1$$

where $\bar{\sigma}$ is the effective stress, $d\,\bar{\varepsilon}$ is effective strain increment and $\bar{\varepsilon}_f$ is the effective strain at fracture (Freudenthal, 1950).

$C_i$ , where i :1,2,... are critical values, calculated by using these criteria

In view of the importance of the largest tensile stress, Cockcroft and Latham have suggested an alternative fracture criterion based on a critical value of the tensile strain energy per unit of volume (Cockcroft, 1968).

$$\int_0^{\bar{\varepsilon}_f} \sigma_{max}\, d\,\bar{\varepsilon} = C_2$$

where $\sigma_{max}$ is the largest (tensile) principal stress

The fracture of ductile solids has been observed to result from the large growth and coalescence of microscopic voids. This dependence guided McClintock to assume that fracture is reached when the spacing between voids in a material reaches a critical value. The fracture criterion derived from this assumption can be written as follows (McClintock, 1968):

$$\int_0^{\bar{\varepsilon}_f} \left[ \frac{\sqrt{3}}{2(n-1)} sinh\left\{ \frac{\sqrt{3}\,(n-1)}{2} \frac{\sigma_a + \sigma_b}{\bar{\sigma}} \right\} + \frac{3}{4} \frac{\sigma_a - \sigma_b}{\bar{\sigma}} \right] d\bar{\varepsilon} = C_5$$

where the symbol n represents the strain-hardening coefficient of the Ludwik-Holomon stress–strain relationship and $\sigma_a$, $\sigma_b$ are the principal stresses in the direction of the greatest and smallest void deformation.

Tensile tests on smooth specimens are carried out to determine the stress–strain behaviour and the ductile fracture characteristics of the alloys. Optical and scanning electron microscopy is used together with fractography to characterise the microstructure of the alloys and to study the damage and fracture mechanisms. Finite element analysis is combined with the experimental results to determine the work-hardening curves of the materials to failure.

## 3. Experimental procedure

In the present paper, the tension test is used to determine the strain to fracture for A7075 aluminum alloys at various temperatures and strain rates.

Nominal chemical composition (in weight %) of aluminum alloy A7075, which was received as extruded bar is : 90% Al; 0,06% Si; 0,19% Fe; 1,3% Cu; 0,04% Mn; 2,4% Mg; 0,19% Cr; 5,7% Zn; 0,08% Ti. The equipment used for the tensile tests is represented in Fig. 1. The dimensions of the tensile specimen are illustrated in Fig. 2. The as-extruded material was annealed at 415 ± 2°C for 2hr and air cooled to room temperature.

The isothermal hot tensile tests were carried out at 300, 350, 400 and 450°C under the strain rates of 0.005 and $0.1s^{-1}$ to study the tensile behavior of the experimental alloy. The specimens were first heated up to the deformation temperature and held isothermally for 5 minutes before straining. This was followed by quenching the specimens in water just after straining. The elongation-to-failure was measured from the gauge length of the fractured specimen.


*Fig.1 Experimental equipment*

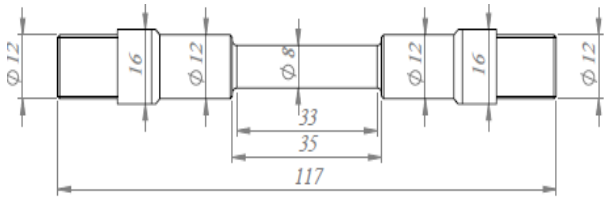


*Fig.2. Dimensions of the tensile specimen.*

## 4. Results and discussions

To determine the aluminum and plastic flow stress of aluminum 7075, a tensile test was performed. The tested specimens after fracture are presented in Fig. 3.


*Fig. 3. Specimens tested in tension : a) initial specimen; b)T= 300 $^0$C, $\dot{\varepsilon}$=0,005 s$^{-1}$; c) T= 350$^0$C, $\dot{\varepsilon}$=0,005 s$^{-1}$, d) T= 400 $^0$C, $\dot{\varepsilon}$=0,005 s$^{-1}$, e) T= 450 $^0$C, $\dot{\varepsilon}$=0,005 s$^{-1}$, f) T= 450$^0$C , $\dot{\varepsilon}$=0,1 s$^{-1}$.*

The typical tensile stress-true strain curves obtained from tensile tests in the temperature range of 300–450ºC under the strain rates of $10^{-3}$ and $10^{-1}$ are shown in Fig.4. The Cauchy stress and the logarithmic strain were calculated as:

$$\sigma = \frac{F}{A}$$

And

$$\delta = ln\frac{A_0}{A}$$

where F is the force, $A_0$ is the initial cross-section area, and A is the final cross-section area of the specimen.

To examine the microstructure evolution and the fracture mechanisms, the specimens were sliced and the cross section in the longitudinal direction of the failed tensile specimens was polished and investigated for the various alloys in the scanning electron microscope.

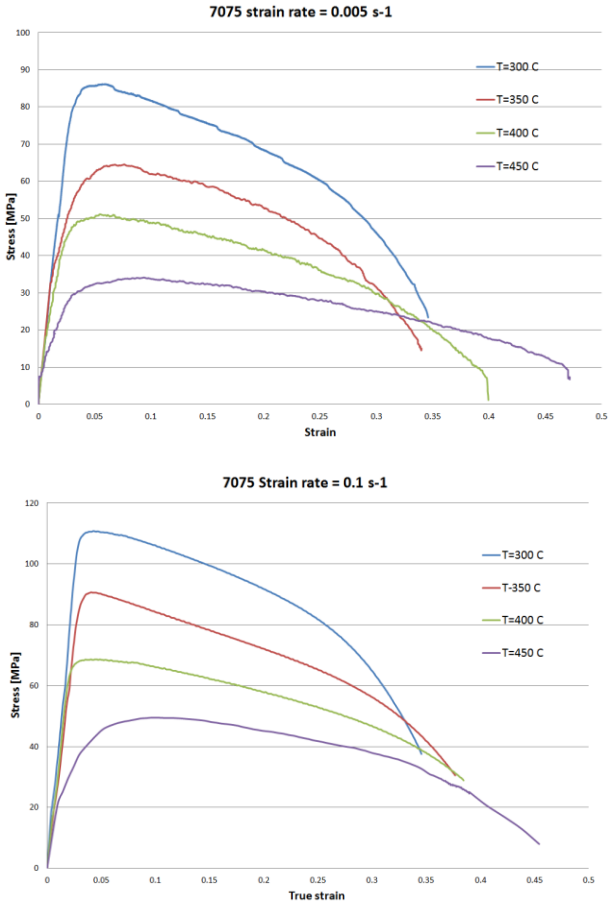


*Fig. 4. Stress- strain curves.*

As is evident, the flow stress characteristics are significantly dependent on the temperature and strain rate.

Typical fracture surfaces of the tensile test specimens are shown in Fig. 5. The macroscopic appearance of the fracture is similar for all the specimens investigated. However, as seen the cross-sectional area at fracture decreases with increasing deformation temperature due to the increase in ductility. The fracture mode is cup-and-cone in all cases, implying that the fracture started from the centre and grew outward towards the edges.

Fig. 6 and 7 shows fractographs of some fractured specimens after tensile tests. The ductile dimples with different size and depth are seen without any cleavage facet on the fracture surfaces. This indicates a ductile fracture mode. As is expected, the observed changes in the fracture surface topography coincide with the ductility variation in ductility–temperature curve, where the contribution of dimpling increases by deformation temperature.

The mechanisms controlling the evolution of damage and the ductile fracture of metallic materials are nucleation, growth and coalescence of microscopic voids [16]. The voids nucleate at constituent particles or inclusions when the stress on the particle is sufficient to induce either particle cracking or particle– matrix decohesion. Continuum models for void nucleation assume that for a given particle size and geometry, the

formation of voids depend on the equivalent stress as well as the hydrostatic stress acting on the particle [17].

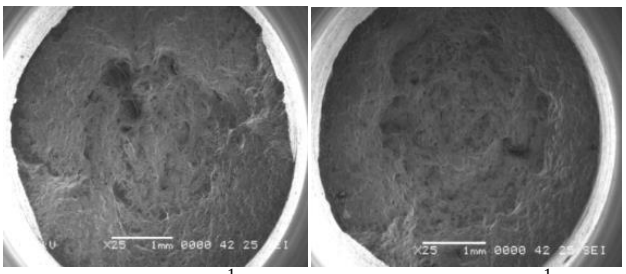

$\dot{\varepsilon}$=0,005 $s^{-1}$, $\dot{\varepsilon}$=0,1 $s^{-1}$

a. T=20 $^0$C

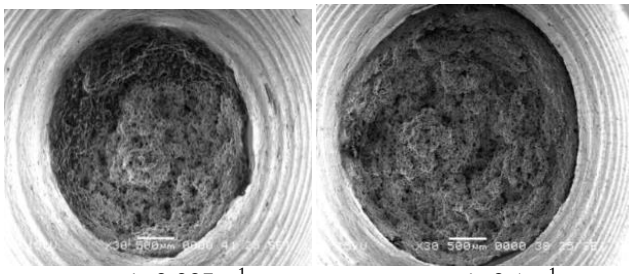

$\dot{\varepsilon}$=0,005 $s^{-1}$ $\dot{\varepsilon}$=0,1 $s^{-1}$

b. T= 300$^0$C

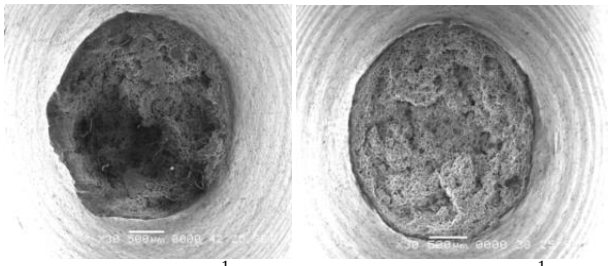

$\dot{\varepsilon}$=0,005 $s^{-1}$ $\dot{\varepsilon}$=0,1 $s^{-1}$

c.T= 350$^0$C

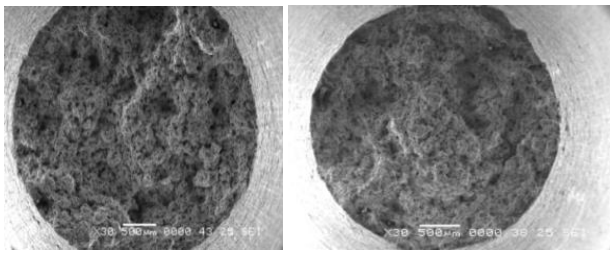

$\dot{\varepsilon}$=0,005 $s^{-1}$ $\dot{\varepsilon}$=0,1 $s^{-1}$

d. T=450$^0$C

*Fig.5. Scanning electron micrographs of surface fracture*.

Void coalescence occurs typically by localised plastic deformation and necking of the ligament between adjacent voids.

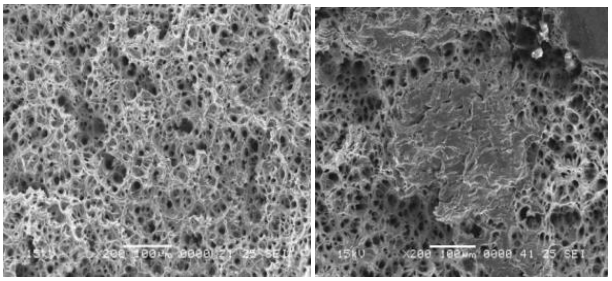

*a.* *b.*

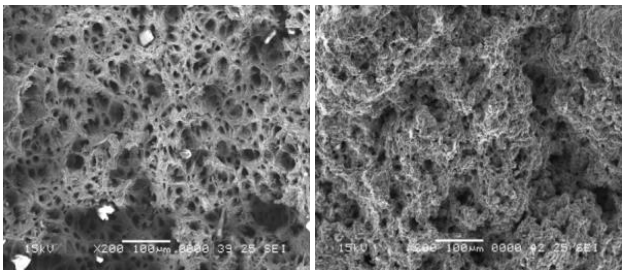

*c.* *d.*

*Fig.6. The SEM images of tensile fracture function of temperature: a)T=la 300$^0$C, b)T=350$^0$C, c)T= 400$^0$C, d)T 450$^0$C; $\dot{\varepsilon}$=0,005 $s^{-1}$.*

It is observed that the fracture surface is covered with two categories of dimples, i.e. a low density of coarse dimples and a higher density of small dimples. The high density of voids and the constituent particles observed at the bottom of several of the voids in the fracture surfaces indicate that void initiation and growth is a major mechanism for fracture. The voids were either nucleated around the constituent particles by decohesion or particle cracking [18].

The fracture surfaces display both large and small dimples which are associated with the constituent particles.

Even if particles were not seen in all the coarse dimples, it cannot be excluded that particles have been present; indeed, the particles may have fallen out during fracture or they may be present in the opposite fracture surface. The size and number density of dimples are linked to the size and density of the constituent particles. Small dimples without particles were also observed in the fracture surface, indicating other possible mechanisms for void coalescence, such as interacting slip planes creating voids in the junction points [19].

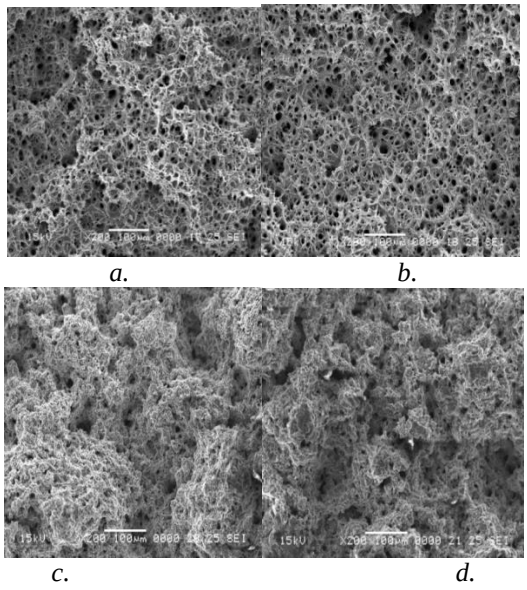

*a.* *b.*

*c.* *d.*

*Fig.7. The SEM images of tensile fracture appearance when: a)T= 300$^0$C, b) T= 350$^0$C, c)T= 400$^0$C, d)T= 450$^0$C; $\dot{\varepsilon}$=0,1 s$^{-1}$*

The damage and failure mechanisms are the same in the alloy, namely nucleation, growth and coalescence of voids, but the strain to failure depends on the yield stress. It is found that the strain to failure decreases with increasing yield stress.

## 5. Simulation details

Forge is a commercial software used for the analysis of plastic deformation processes. The program is based on the finite element method for cold and hot metal forming. It enables the thermo-mechanical simulation of the plastic deformation processes of metals in an axisymmetric, homogeneous and isotropic state of deformation and obeys the von Mises criterion. The calculations of the metal flow, stress field, strain, strain rate and temperature are conducted on the assumption of the viscoplastic model of the deformed body .

The geometries of the billet and dies were generated in SolidWorks and the meshes within their space domains in Forge3D. After the model had been created, a number of simulations were run to study the effect of temperature and strain rate on the metal flow and deformation parameters

The distribution of the effective stress inside the billet and the damage value obtained with the normalized C & L ductile fracture criterion, at a particular stage of traction was determined by the simulation model (Fig.8, Fig.9).

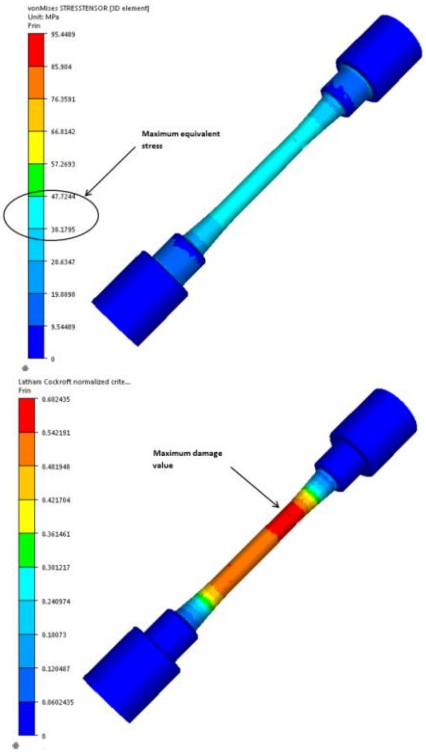


*Fig. 8. The 7075 aluminum effective stress diagram and damage value,T=450$^0$C, $\dot{\varepsilon}$=0,005 s$^{-1}$.*

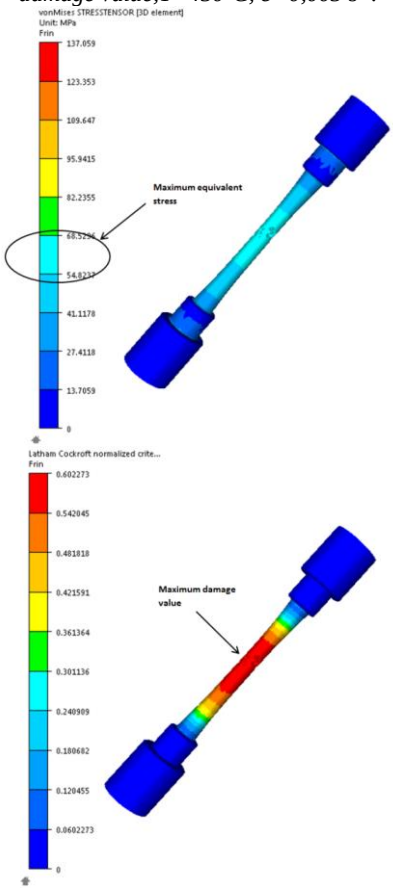


*Fig. 9. The 7075 aluminum effective stress diagram and damage value, T=450$^0$C, $\dot{\varepsilon}$=0,1 s$^{-1}$.*

The damage value for the 7075 aluminum alloy, obtained when the normalized C & L criterion

had a C value of 0.542. A damage value over 0.542 would produce grid separation (fracture), resulting in fracture of the specimen.

In Fig.10 are presented the experimental and simulated stress-strain curves that were obtained for different strain rates.

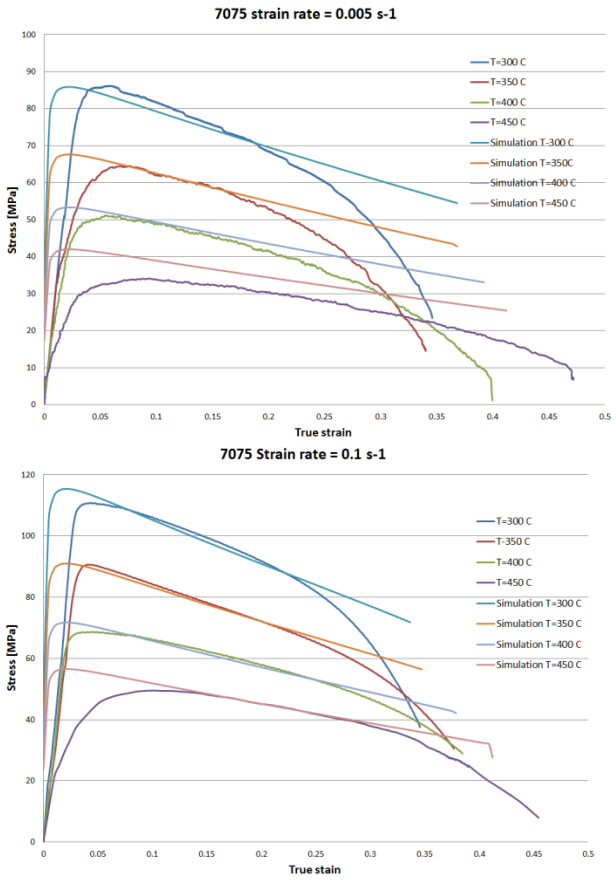


*Fig.10. Experimental and simulated stress-strain curves.*

## 6. Conclusions

As one of the principal failures, ductile fracturing restricts metal forming process. The fracture of ductile solids has frequently been observed to result from the large growth and coalescence of microscopic voids, a process enhanced by the superposition of hydrostatic tensile stresses on a plastic deformation field. Aluminum alloy 7075 have been tested under uniaxial tensile conditions at various temperatures and strain rates to determine the strain to fracture. The fracture modes of the alloys is characterised by scanning electron microscopy. The tensile test shows that by increasing temperature, ductility had an ascending trend. This was justified considering the fact that the volume fractions of the second phase particles might decrease at higher temperature thereby their detrimental effects on cavity nucleation and growth would be decreased. Moreover, factors affecting ductile fractures, such as stress, strain, and damage value were analyzed.

True stress-strain values were obtained from tensile tests of 7075 aluminum by performing a finite element simulation analysis. The normalized Cockcroft and Latham ductile fracture criterion used in the finite element analysis shown the critical damage value for the studied material.

## References

[1] M. Rajamuthamilselvan, S. Ramanathan, Journal of Alloys and Compounds 509 (2011) 948–952
[2] C.M.A. Silva, L.M. Alves, C.V. Nielsen, A.G. Atkins, P.A.F. Martins, Journal of Materials Processing Technology **215,** 287 (2015).
[3] M.R. Rokni, A. Zarei-Hanzaki, Ali A. Roostaei, H.R. Abedi, Materials and Design **32,** 2339 (2011).
[4] Williams James C, Starke Jr Edgar A. Acta Mater **59,** 5775 (2003).
[5] M.R. Rokni, A. Zarei-Hanzaki, Ali A. Roostaei, H.R. Abedi, Materials and Design **32,** 2339 (2011).
[6] H Zhang, L Li, D Yuan, D. Peng, Materials Characterisation **58,** 168 (2007).
[7] O. A. Ketill, B. Pedersen, A. C. Tore Børvik, Materials and Design **32,** 97 (2011).
[8] RE. Zinkham, Eng Fract Mech **1,** 275 (1968).
[9] TS Srivatsan, G Guruprasad, VK. Vasudevan, Materials Design **29**, 742 (2008).
[10] JE. Hatch, Aluminium: properties and physical metallurgy. American society for metals. Ohio: Metals Park; 1984
[11] Y Chen, KO Pedersen, AH Clausen, OS Hopperstad. Materials Science Engineeering A **523,** 253 (2009).
[12] R.H. Wagoner, K.S. Chan, S.P. Keeler (Eds.), Forming Limit Diagrams: Concepts, Methods, and Applications, TMS, Warrendale, 1989
[13] P.W. Bridgman, Studies in Large Plastic Flow and Fracture, McGraw- Hill, New York, 1952
[14] Dyi-Cheng Chen, Ci-Syong You, Fu-Yuan Gao, Procedia Engineering **81,** 1252 (2014 ).
[15] Ozgür Koçak , Aanalysis of the formability of metals, MSc Thesis, 2013
[16] A.A. Benzerga, J.-B. Leblond, Adv. Appl. Mech. **44,** 169 (2010).
[17] T.L. Anderson, Fracture Mechanics. Fundamentals and Applications, third ed. Taylor & Francis, 2005
[18] E Maire, S Zhou, J Adrien, M. Dimichiel, Eng. Fract. Mech. **78**, 2679 (2011).
[19] KO Pedersen, HJ Roven, O-G Lademo, OS. Hopperstad, Materials Science Engineering A **473,** 81 (2008).

*Corresponding author: mariana.pop@ipm.utcluj.ro